Separation Science and Technology
Publication details, including instructions for authors and subscription information:
http://www.informaworld.com/smpp/title~content=t713708471

Deposition of small particles on spherical collectors under turbulent flow conditions

Hasan A. Mousa[a]
[a] Department of Chemical Engineering, Jordan University of Science and Technology, Irbid, Jordan

Online publication date: 13 June 2002

To cite this Article Mousa, Hasan A.(2002) 'Deposition of small particles on spherical collectors under turbulent flow conditions', Separation Science and Technology, 37: 9, 2021 — 2035
To link to this Article: DOI: 10.1081/SS-120003499
URL: http://dx.doi.org/10.1081/SS-120003499

SEPARATION SCIENCE AND TECHNOLOGY, 37(9), 2021–2035 (2002)

DEPOSITION OF SMALL PARTICLES ON SPHERICAL COLLECTORS UNDER TURBULENT FLOW CONDITIONS

Hasan A. Mousa*

Department of Chemical Engineering, Jordan University of Science and Technology, P.O. Box 3030, Irbid 22110, Jordan

ABSTRACT

A model describing the deposition rate of small particles on spherical collectors under turbulent flow conditions was derived. The derivation was based on several assumptions, the most important ones being that the small particles occupy an area equal to its projected area on the surface of the collectors and no detachment takes place. Three cases were considered: the small and the collector particles are both monodisperse in size (case I), the small particles are polydisperse while the collector particles are monodisperse (case II) and finally the small and the collector particles are both polydisperse in size (case III). The log normal distributions were used to represent the polydisperse sizes.

INTRODUCTION

Many industrial processes produce effluent streams (mainly water) that contain suspended small particles of different nature. The size of such small

*Fax: 962-2-7095044; E-mail: akras@just.edu.jo

particles ranges from a few nanometers to several hundred microns. The removal of such suspended solids may be accomplished by many separation techniques such as adsorption, filtration, flotation, or settling. For example, in paper recycling industry, flotation along with washing is used to remove ink particles (1–5). In water and wastewater treatment, filtration, settling, and adsorption techniques are used (6).

An alternative technique is to collect the suspended small particles on the surface of collector particles (7–9). Deposition of various types of colloidal particles on solid collectors has been studied extensively in literature. An excellent review on particle transfer to solid surfaces can be found in Refs. (10,11). Kamiti and van de Ven (12) and Xia et al. (13) used the impinging jet technique to study the deposition of colloidal particles on glass surfaces. Clay and calcium carbonate deposition on pulp fibers was studied (14–16).

Several attempts were made to model deposition of colloidal particles under various flow conditions. Al-Jabari et al. modeled the flow and the deposition of filler particles in packed beds of pulp fibers (17). Petlicki and van de Ven theoretically studied the deposition of colloidal particles on spheroids in simple shear flow (18). Mousa studied the deposition of colloidal particles on solid spheres under simple shear flow conditions (19). In this article, the deposition of spherical particles on spherical collector particles under turbulent flow conditions will be described. The development will consider three cases: the spherical and the collector particles are monodisperse in size (case I); the spherical particles are polydisperse while the collector particles are monodisperse (case II), and both the spherical and the collector particles are polydisperse (case III).

THEORETICAL DEVELOPMENT

Consider a suspension containing certain small particles and collector particles. The small and the collector particles are assumed spherical in shape of mean diameters d and D, respectively such that $D > d$. The number of the small and the collector particles per unit volume is n and N, respectively. Upon subjecting the suspension to a stirring action, the small and the collector particles will collide with each other. This will lead to the deposition of the small particles on the surface of the collector particles. The rate of deposition of the small particles is equal to the rate of change of the total number of the small particles, $-\mathrm{d}n/\mathrm{d}t$, remains suspended. To derive an expression for $\mathrm{d}n/\mathrm{d}t$, the following assumptions will be made: first, the bonding between the small and the collector particles is strong so that no detachment takes place. This is valid in systems where surfactant is added to enhance deposition or in the case where the small and the collector particles have opposite charges. Second, the small particles are stable and they do not coagulate. Hence, the decrease in the number of small particles is only due to its deposition on the collector's surface. Third, the small particles form monolayer coverage on the collector's surface. This assumption is a consequence of the second assumption since the small particles are stable and have no affinity for each other. Fourth, low area coverage is assumed so that the small particles have equal access to the collector's surface regardless of its size. Finally, the deposition efficiency of the small particles is independent of its size. A mass balance on a unit volume of the suspension shows that (20)

$$\mathrm{d}n/\mathrm{d}t = -\upsilon\alpha(1 - \theta) \tag{1}$$

where t is the time, υ the collision frequency between the small and the collector's particles, θ the fractional area coverage, i.e., the fraction of the total surface area of the collector covered with the small spheres to the total surface area of the collector particles, and α the collision efficiency defined as the number of collisions that lead to deposition (successful collisions) to the total number of collisions. The following analysis will consider three cases: case I, both the small and the collector particles are monodisperse in size; case II, the small particles are polydisperse whereas the collector particles are monodisperse; case III, both the collector and the small particles are polydisperse.

Case I: Monodisperse Small Particles

The collision frequency between a small particle of size v and a collector particle of size V in stirred vessel can be written as (20,21)

$$\upsilon = \left(\frac{9\pi}{2}\right)^{1/3}(v^{2/3} + V^{2/3})(\bar{u}^2(v) + \bar{U}^2(V))^{1/2}nN \tag{2}$$

where $\bar{u}^2(v)$ and $\bar{U}^2\,(V)$ are the mean square fluctuation velocities of particles of volume v and V, respectively (20). For isotropic fluids in which $Re > 10{,}000$ (where Re is the Reynolds number based on the vessel diameter), $\bar{u}$ and $\bar{U}$ are given by

$$\bar{u}^2 = K\varepsilon^{2/3}v^{2/9} \tag{3}$$

$$\bar{U}^2 = K\varepsilon^{2/3}V^{2/9} \tag{4}$$

In Eqs. (3) and (4), K is a constant (21,22) and ε the distribution of energy dissipation given (21–24).

$$\varepsilon = C\omega^3L^2 \tag{5}$$

where ω is the stirrer speed, L the impeller diameter, and C a constant that depends on the geometry of the vessel and the agitator. Combining Eqs. (1)–(5), noting that $v = \pi d^3/6$ and $V = \pi D^3/6$ results in the following equation

$$\frac{\mathrm{d}n}{\mathrm{d}t} = -C_1[d^2 + D^2][d^{2/3} + D^{2/3}]^{1/2} nN\alpha(1 - \theta) \tag{6}$$

where $C_1 = 3K^{1/2}(\pi/6)^{10/9}\varepsilon^{1/3}$.

The area coverage can be related to n as follows. Let n_0 be the number of small spheres per unit volume at $t = 0$. Moreover, let n_s be the number of small spheres deposited on the surface of the collector per unit volume. At any time, it can be written that

$$n_0 = n + n_s \tag{7}$$

Assuming that each particle occupies an area equal to its projected area, $\pi d^2/4$, on the surface of the collector particle, then

$$\theta = \frac{\text{Area covered by the solid spheres}}{\text{Total surface area of the collector particles}} = \frac{d^2 n_s}{4D^2N} = \frac{d^2(n_0 - n)}{4D^2N} \tag{8}$$

Let $n^* = n/n_0$, $t^* = C_1[d^2 + D^2][d^{2/3} + D^{2/3}]^{1/2}\alpha Nt$ and $C_2 = d^2 n_0/4D^2N$, then Eq. (6) can be rewritten as

$$\frac{\mathrm{d}n^*}{\mathrm{d}t^*} = -n^*[1 - C_2 + C_2 n^*] \tag{9}$$

The solution of Eq. (9) is

$$n^* = \begin{cases} \dfrac{1 - C_2}{\exp[(1 - C_2)t^*] - C_2}, & C_2 \neq 1 \\ \dfrac{1}{t^* + 1}, & C_2 = 1 \end{cases} \tag{10}$$

Note that Eq. (10) is similar to an equation derived by Mousa (19) for deposition in simple shear flow.

Case II: Polydisperse Small Particles

Consider that the small particles are polydisperse in size and can be represented by a log normal distribution of mean size d_m and a standard deviation σ_m. Dividing this distribution into classes of size d_i and number n_i, then the collision frequency of particles in class i with the collector particles, υ_i, and the area coverage, θ, are given by

$$\upsilon_i = \left(\frac{9\pi}{2}\right)^{1/3} (v_i^{2/3} + V^{2/3})(\bar{u}_i^2(v_i) + \bar{U};^2 (V))^{1/2} n_i N \tag{11}$$

$$\theta = \frac{n_0}{4N} \sum_{i=1}^{I} d_i^{*\,2} (n_{0,i}^* - n_i^*) \tag{12}$$

where $d_i^* = d_i/D$, $n_{0,i}^* = n_{0,i}/n_0$ is the number of the small particles in class i at $t = 0$, n_0 is the total number of small particles at $t = 0$ such that $n_0 = \sum_i^I n_{0,i}$, $\mathrm{n}_i^* = n_i/n_0$ and I is the total number of classes. Utilizing Eqs. (11) and (12) and summing over I, the change of the total number in this case becomes

$$\begin{aligned} \frac{\mathrm{d}n^*}{\mathrm{d}t^*} &= \frac{\mathrm{d}\sum_{i=1}^{I} n_i^*}{\mathrm{d}t^*} \\ &= -\left\{ \sum_i^I (d_i^{*2} + 1)(d_i^{*2/3} + 1)^{1/2} n_i^* \right\} \\ &\quad \times \left\{ 1 - C_3 \sum_i^I d_i'^2 (n_{0,i}^* - n_i^*) \right\} \end{aligned} \tag{13}$$

In Eq. (13), $C_3 = n_0/4N$ and $t^* = C_1 D^{7/3} N\alpha t$.

Case III: Polydisperse Small and Collector Particles

Assume that the small and the collector particles are both polydisperse and are log-normally distributed with a mean size and standard deviation of d_{m} and σ_{m} and D_c and σ_{c}, respectively. Then the collision frequency between a small particle in class i with a collector particle in class j, υ_{ij} and the area coverage, θ are given by

$$\upsilon_{ij} = \left(\frac{9\pi}{2}\right)^{1/3} (v_i^{2/3} + V_j^{2/3})(\bar{u}_i^2(v_i) + \bar{U}_j^2(V_j))^{1/2} n_i N_j \tag{14}$$

$$\theta = C_3 \frac{\sum_{i=1}^{I} d_i^{*2} (n_{0,i}^* - n_i^*)}{\sum_{j=1}^{J} D_j^{*2} N_j^*} \tag{15}$$

The change of the total number of small particles using Eqs. (14) and (15) becomes

$$\frac{\mathrm{d}n^*}{\mathrm{d}t^*} = \frac{\mathrm{d}\sum_{i=1}^{I} n_i^*}{\mathrm{d}t^*}$$
$$= \left\{ \sum_{i}^{I} \sum_{j}^{J} (d_i^{*2} + D_j^{*\prime 2})(d_i^{*2/3} + D_j^{*2/3})^{1/2} n_i^* N_j^* \right\}$$
$$\times \left\{ 1 - C_3 \frac{\sum_{i=1}^{I} d_i^{*2}(n_{0,i}^* - n_i^*)}{\sum_{j=1}^{J} D_j^{*2} N_j^*} \right\} \qquad (16)$$

where $d_i^* = d_i/D_c$, $D_j^* = D_j/D_c$, $N_j^* = N_j/N$, $t^* = C_1 \alpha D_c^{7/3} N t$ and J is the total number of classes of the collector particles.

RESULTS AND DISCUSSION

The change in the total number of the monodisperse small particles that remain suspended in the liquid vs. the dimensionless time for various values of C_2 is shown in Fig. 1. As expected, the total number of the small particles decreases

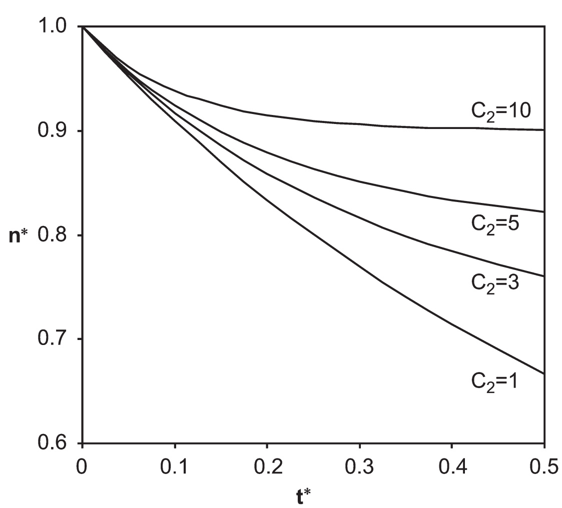

Figure 1. A plot of n^* vs. t^* for monodisperse small particles of 50 μm in diameter for various values of C_2. The collector particles are monodisperse of diameter = 1500 μm.

continuously until no more deposition can take place. The figure also shows that larger the value of C_2, slower is the decrease in n^*. This is because the initial number of the spherical particles is larger as the value of C_2 is larger. Hence, the driving force for deposition is higher and therefore the collector surface is covered faster with the spherical particles. Alternatively large values of C_2 means that the number of the small particles is large compared to the collector particles and hence small surface area to cover. The same behavior was observed for case II as can be seen in Fig. 2. The spherical particles in this case are represented by a log-normal distribution of mean diameter 50 μm and a standard deviation of 0.3. The diameter of the collector particles is 1500 μm. Similar behavior was obtained for case III as can be seen in Fig. 3. In this case, both the small and the collector particles are represented by log-normal distributions. The mean diameter and the standard deviation of the small particles are 10 μm and 0.3, respectively. For the collector particles, the mean diameter and the standard deviation are 1500 μm and 0.3, respectively. The fractional area coverage for the above three cases are shown in Figs. 4–6, respectively. To show the change in the distribution of the spherical particles as deposition proceeds, the particle size distribution at various values of t^* and for the case where $C_3 = 1000$ is plotted in Fig. 7. As can be seen from Fig. 7, the number of particles, n_i^*, of any diameter d_i decreases

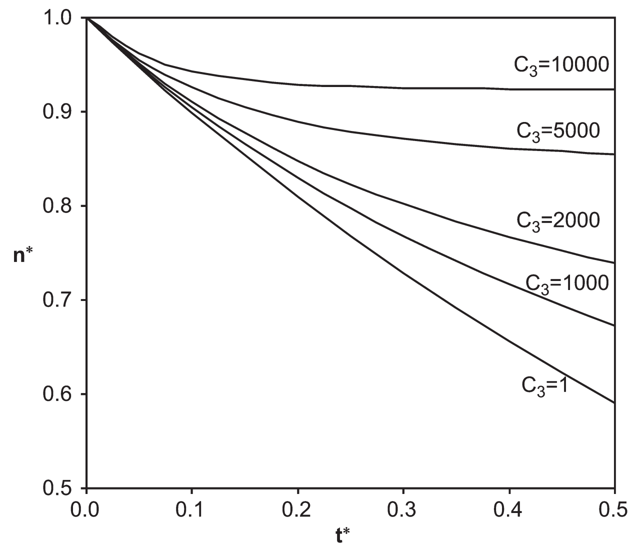

Figure 2. A plot of n^* vs. t^* for log-normally distributed small particles of mean diameter = 50 μm and a standard deviation of 0.3 for various values of C_3. The collector particles are monodisperse of diameter = 1500 μm.

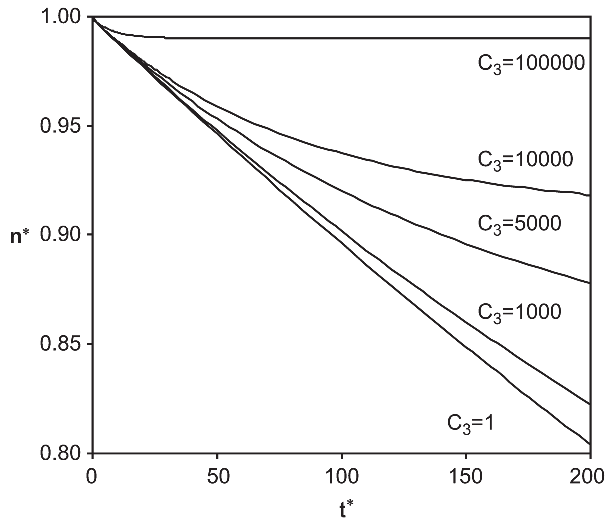

Figure 3. A plot of n^* vs. t^* for log-normally distributed small particles of mean diameter $= 50\,\mu$m and a standard deviation of 0.3 for various values of C_3. The collector particles are log-normally distributed with a mean diameter of $1500\,\mu$m and a standard deviation of 0.3.

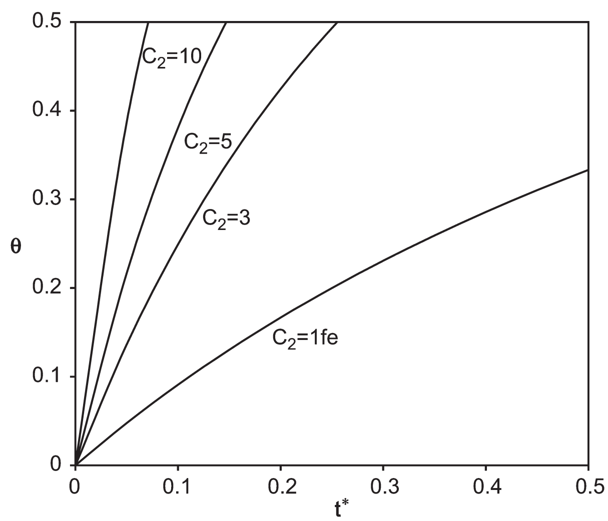

Figure 4. A plot of the area coverage, θ vs. t^* for monodisperse small particles of $50\,\mu$m in diameter for various values of C_2. The collector particles are monodisperse of diameter $= 1500\,\mu$m.

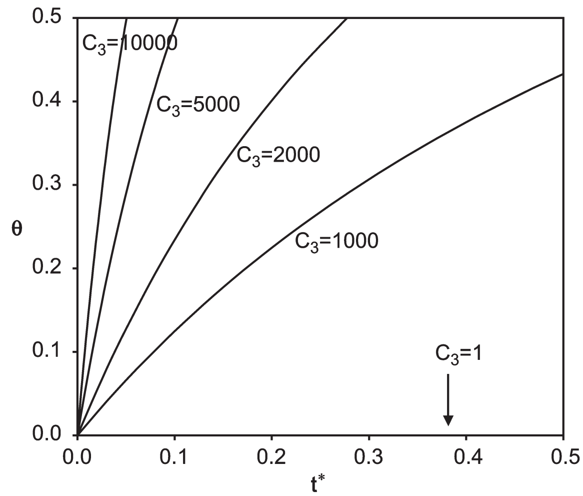

Figure 5. A plot of the area coverage, θ vs. t^* for log-normally distributed small particles of mean diameter = 50 μm and a standard deviation of 0.3 for various values of C_3. The collector particles are monodisperse of diameter = 1500 μm.

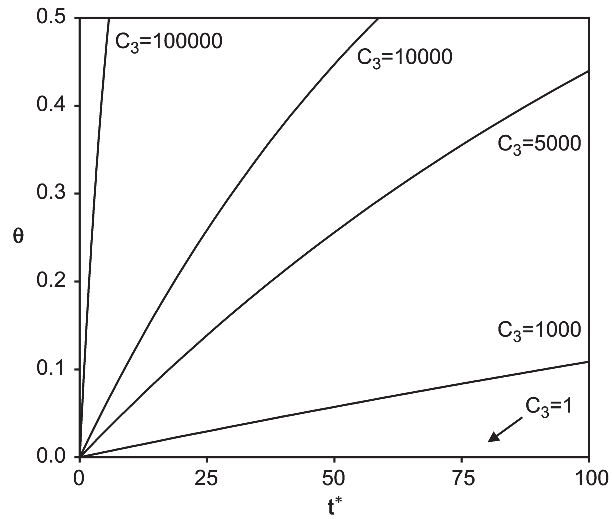

Figure 6. A plot of the area coverage, θ vs. t^* for log-normally distributed small particles of mean diameter = 50 μm and a standard deviation of 0.3 for various values of C_3. The collector particles are log-normally distributed with a mean diameter = 1500 μm and a standard deviation of 0.3.

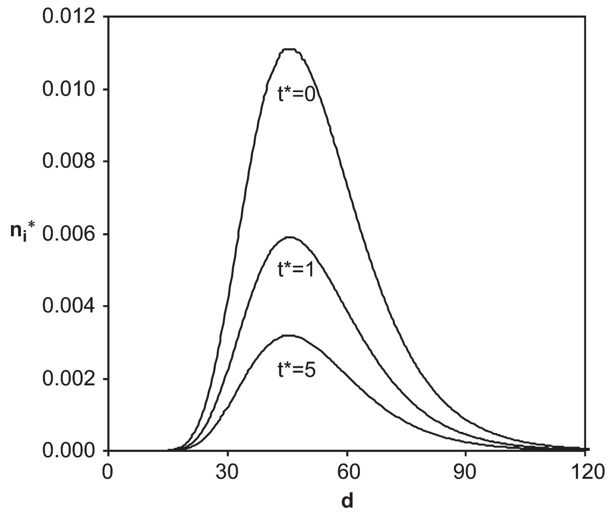

Figure 7. The change in the size distribution of the small particles for various values of t^*. The initial distribution of the small particles is log normal with a mean diameter of $50\,\mu$m and a standard deviation of 0.3. The collector particles are monodisperse of diameter $= 1500\,\mu$m. The value of C_3 is 1000.

continuously with time. The decrease is faster as the initial number is larger and the maximum change being around the particles that have the highest probability (around the mean). This is because the collision frequency is proportional to the number of the particles (see Eqs. (2), (11), or (14)).

The effect of the mean spherical particle diameter on the rate of deposition for case II is shown in Fig. 8. The number of spherical particles vs. t^* for the case where the mean diameters are 10, 30, and $50\,\mu$m are plotted in Fig. 8. The standard deviation for the three distributions is 0.3, the value of $C_3 = 2000$ and $D = 1500\,\mu$m. As can be noticed from Fig. 8, the smaller mean diameter possesses the faster rate. This is because the geometrical area of a small particle is small too. Hence, large number of the small particles is needed to cover a given surface area of the collectors compared to the large particles, therefore its number drops faster. The same result was obtained for the case where the collector particles are polydisperse as can be seen in Fig. 9.

The effect of the collector diameter on the deposition rate for case II where the small particles are polydisperse with mean diameter of $50\,\mu$m, a standard deviation of 0.3, and $C_3 = 2000$ is shown in Fig. 10. As can be noticed from Fig. 10, the larger the mean diameter the faster is the deposition rate. The reason for this is that the larger the collector diameter the larger is the available area for

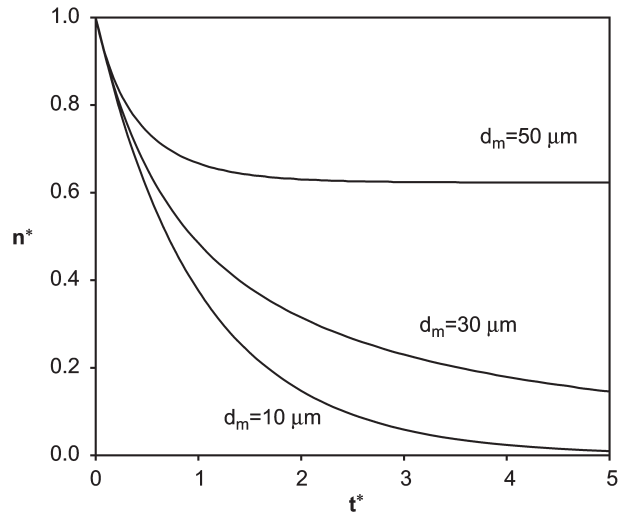

Figure 8. The effect of the mean diameter of the small particles on the change of n^* vs. t^*. The small particles are log-normally distributed with a standard deviation of 0.3 and a mean diameter as indicated in the figure. The collector particles are monodisperse of diameter $= 1500\,\mu$m. The value of C_3 is 2000.

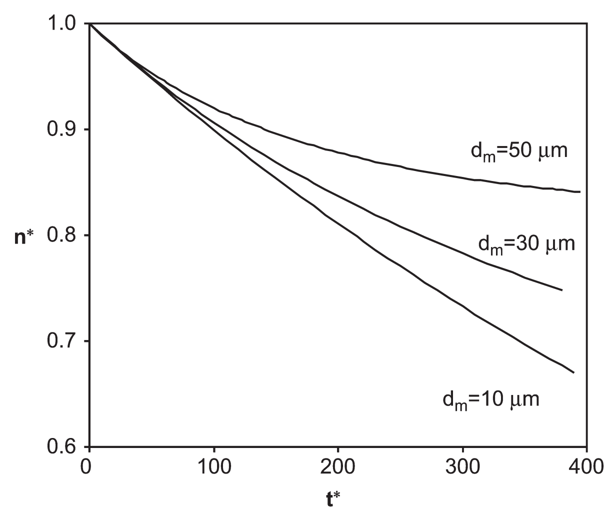

Figure 9. The effect of the mean diameter of the small particles on the change of n^* vs. t^*. The small particles are log-normally distributed with a standard deviation of 0.3 and a mean diameter as indicated in the figure. The collector particles are log-normally distributed with a mean diameter of 1500 μm and a standard deviation of 0.3. The value of C_3 is 5000.

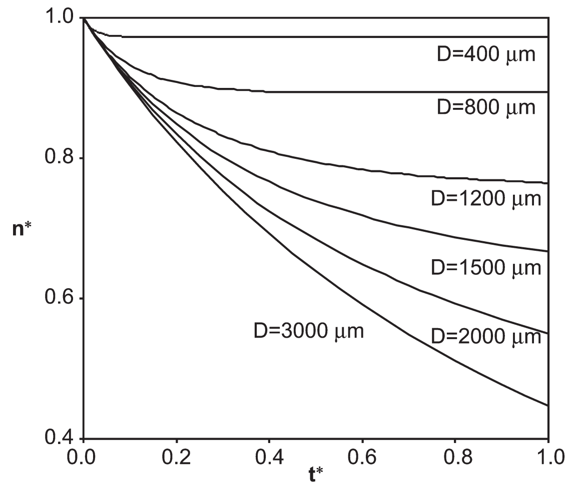

Figure 10. The effect of the monodisperse collector mean particle diameter on the change of n^* vs. t^*. The small particles are log-normally distributed with a mean size of 50 mm and a standard deviation of 0.3. The value of C_3 is 2000.

deposition and hence more small particles are lost from the suspension by depositing on the collectors' surface.

It is worth mentioning that the deposition efficiency can be determined by comparing theoretically the calculated values of n^* vs. t^* with experimentally measured values of n vs. t. Thus, by knowing the initial distribution and the mean diameter of the small and the collector particles and to the operating conditions, the value of α can be estimated (19,25).

It should be noted that turbulence enhances deposition due to the following reasons: firstly, the collision frequency (number of collisions per unit time per unit volume) increases since the later is proportional to the rotational speed. This gives the particles (the small and the collector ones), a higher chance to meet. Secondly, in turbulent flow the small particles attain larger kinetic energy; hence they can overcome the energy barrier, which enhances deposition. Thirdly, the collision efficiency, α, is proportional to the rotational speed (21) whereas in simple shear, α decreases as the shear rate increases (26).

CONCLUSIONS

Theoretical expressions describing the loss of small particles by deposition on collector particles in turbulent flow have been derived. The study considered three cases: monodisperse, small, and collector particles (case I), the small particles are polydisperse whereas the collector particles are monodisperse (case II), and the small and the collector particles are both polydisperse (case III). The results showed that higher deposition rates results when the mean diameter of the small particles gets smaller and when the mean diameter of the collector particles gets larger.

NOMENCLATURE

C	constant, dimensionless
C_1	constant, dimensionless
C_2	constant, dimensionless
C_3	constant, dimensionless
d	solid particle diameter (m)
d_{m}	mean diameter of the solid particles (m)
D	collector particle diameter (m)
D_{c}	mean diameter of the collector particles (m)
K	constant used in Eqs. (3) and (4), dimensionless
L	impeller diameter (m)
n	number of suspended particles/unit volume (m^{-3})
n_0	number of suspended particles/unit volume at $t = 0$, (m^{-3})
n_{s}	number of solid particles deposited on the collector surface/unit volume (m^{-3})
N	number of collector particles/unit volume (m^{-3})
Re	Reynold's number based on the vessel diameter, dimensionless
t	time (sec)
$\bar{u}^2(v)$	mean square velocity of particle of volume v (m/sec)
$\bar{U}^2(V)$	mean square velocity of particle of volume V (m/sec)
v	volume of the solid particle (m^3)
V	volume of the collector particle (m^3)

Greek Letters

α	collision (deposition) efficiency, dimensionless
ε	energy dissipation (J/kg-sec)
σ_{c}	standard deviation of the log-normally distributed collector particles, dimensionless
σ_{m}	standard deviation of the log-normally distributed spherical particles, dimensionless
θ	area coverage, dimensionless
υ	collision frequency, (1/sec)
ω	stirring speed, (1/sec)

Subscript and Superscript

0	initially at $t = 0$
i,j	class I or j
*	dimensionless parameter

REFERENCES

1. Koffinke, R.A. Modern Newsprint Systems Combines Flotation and Washing Deinking. Tappi J. **1985**, *68*, 61–63.
2. Pfalzer, L. Deinking of Secondary Fibers: A Comparison of Washing and Flotation. Tappi J. **1980**, *63*, 113–116.
3. Crow, D.R.; Secor, R.F. The Ten Steps of Deinking. Tappi J. **1987**, *70*, 101–106.
4. Shrinath, A.; Szewczak, J.T.; Brown, I.J. A Review of Ink-Removal Techniques in Current Deinking Technology. Tappi J. **1991**, *74*, 85–93.
5. Zabala, J.M.; McCool, M.A. Deinking at Papelera Peninsular and the Philosophy of Deinking System Design. Tappi J. **1988**, *71*, 62–68.
6. Droste, R.L. *Theory and Practice of Water and Wastewater Treatment*; John Wiley and Sons Inc.: New York, 1997.
7. Mousa, H.; Qasaimeh, M. Experimental Investigation of the De-inking of Recycled Newspaper Using Plastic Particles. Sep. Sci. Technol. **1996**, *31*, 1093–1104.
8. Al-Jabari, M.E.; Mousa, H.; Al-Khateeb, I. Kinetics of Deposition of Carbon Particles on Plastic Particles. Sep. Sci. Technol. **2002**, In press.
9. Mousa, H.; Al-Jabari, M.; Al-Khateeb, I. Effect of Physicochemical Hydrodynamic Conditions on Kinetics of Carbon Particle Deposition on Plastic Spheres. Chem. Eng. J. **2002**, In press.
10. Adamczyk, Z.; Dabros, T.; Czarnecki, J.; van de Ven, T.G.M. Particle Transfer to Solid Surfaces. Adv. Colloid Interface Sci. **1983**, *19*, 183–252.
11. van de Ven, T.G.M. The Capture of Colloidal Particles on Surfaces and in Porous Material: Basic Principles. Colloids Surf. **1998**, *138*, 207–216.
12. Kamiti, M.; van de Ven, T.G.M. Impinging Jet Studies of the Kinetics of Deposition and Dissolution of Calcium Carbonate Particles. Colloids Surf. **1995**, *100*, 117–129.
13. Xia, Z.; Goldsmith, H.L.; van de Ven, T.G.M. Kinetics of Specific and Nonspecific Adhesion of Red Blood Cells on Glass. Biophysics **1993**, *65*, 1073–1083.
14. van de Ven, T.G.M. Particle Deposition on Pulp Fibers. Nordic Pulp Paper Res. J. **1993**, *8*, 130–134.

15. Al-Jabari, M.; van Heiningen, A.R.P.; van de Ven, T.G.M. Experimental Study of Deposition of Clay Particles in Packed Beds of Pulp Fibers. J. Pulp Paper Sci. **1994**, *20*, J289–J295.
16. Kamiti, M.; van de Ven, T.G.M. Kinetics of Deposition of Calcium Carbonate onto Pulp Fibers. J. Pulp Paper Sci. **1994**, *20*, J199–J205.
17. Al-Jabari, M.; van Heiningen, A.R.P.; van de Ven, T.G.M. Modeling the Flow and the Deposition of Fillers in Packed Beds of Pulp Fibers. J. Pulp Paper Sci. **1994**, *20*, J249–J253.
18. Petlicki, J.; van de ven, T.G.M. Shear Induced Deposition of Colloidal Particles on Spheriods. J. Colloid Interface Sci. **1992**, *148*, 14–22.
19. Mousa, H. Modeling the Deposition of Colloidal Particles on Solid Spheres. Sep. Sci. Technol. **1997**, *32*, 3037–3049.
20. Yang, R.T.; Gas Separation by Adsorption Processes, Butterworths: Boston, MA, 1987;.
21. Coulaloglou, C.A.; Tavlarides, L.L. Description of Interaction Processes in Agitated Liquid–Liquid Dispersions. Chem. Eng. Sci. **1977**, *32*, 1289–1297.
22. Kumar, S.; Kumar, R.; Gandhi, K.S. A New Model for Coalescence Efficiency of Drops in Stirred Dispersions. Chem. Eng. Sci. **1993**, *48*, 2025–2038.
23. McCabe, W.L.; Smith, J.C.; Harriott, P. *Unit Operations of Chemical Engineering*, 4th Ed.; McGraw Hill: New York, 1985; 208–252.
24. Coulson, J.M.; Richardson, J.F. *Chemical Engineering*, 3rd Ed.; 1978; Vol. 2, 585–598.
25. Mousa, H.; van de Ven, T.G.M. Stability of Water-in-Oil Emulsions in Simple Shear Flow: 1. Determination of the Orthokinetic Coalescence Efficiency. Colloids Surf. **1991**, *60*, 19–38.
26. van de Ven, T.G.M.; Mason, S.G. The Microrheology of Colloidal Dispersions VII. Orthokinetic Doublet Formation of Spheres. Colloid Polym. Sci. **1977**, *255*, 468–479.

Received May 2001
Revised October 2001